

Department of Chemical Engineering
University of California, Santa Barbara

CH E 180B. Chemical Engineering Laboratory

**Evaluating the Feasibility of Separating and
Recovering Valuable Hydrocarbons
(cyclohexane, heptane, and toluene) from a
Waste Stream using a 21 Stages Distillation
Column**

Sean Shen, Yulun Wu, Chang Yuan

Group 9W

Experiment Conducted between February 5th and February 19th, 2025

Report Submitted on February 26th, 2025

1 Abstract

The transition from batch to continuous processing in chemical manufacturing enhances efficiency, scalability, and process control. This study examines viability of producing sodium acetate (NaAc) from ethyl acetate (EtAc) waste streams through saponification with sodium hydroxide (NaOH) from batch reactor to a Continuous Stirred Tank Reactor (CSTR). The second-order rate law was confirmed, yielding an activation energy $E_a = (33.0 \pm 1.2) \text{ kJ/mol}$, and a pre-exponential factor $A = (3.8 \pm 0.3) \times 10^4 \text{ s}^{-1}$, calculated using the Arrhenius equation. Following the kinetic analysis, the CSTR performance was assessed under varying flow rates ($Q = 100, 200, 300 \text{ mL/min}$) with a mean residence time of $(259.1 \pm 5 \text{ s}, 254.2 \pm 5 \text{ s}, 219.1 \pm 5 \text{ s})$ respectively. Residence Time Distribution (RTD) analysis revealed back-mixing effects, particularly at lower flow rates, influencing conversion efficiency. The conversion exhibited a nonlinear dependence on residence time, with a maximum observed conversion of $33.51 \pm 0.15\%$ at $Q = 200 \text{ mL/min}$. This study provides quantitative insights into the relationship between residence time, flow rate, and reaction kinetics, contributing to the optimization of continuous saponification processes. The findings guide reactor design and scale-up for efficient sodium acetate production while maintaining process control.

Introduction

Distillation is a fundamental separation process in chemical engineering, where components are separated based on differences in boiling points and relative volatilities. This experiment focuses on a ternary distillation column separating a waste stream mixture of cyclohexane, heptane, and toluene. The objective is to maximize cyclohexane recovery while maintaining a minimum purity of 80 wt.%. This requires analyzing vapor-liquid equilibrium (VLE), stage-wise mass balances, and key column operating principles, such as reflux ratio and feed stage placement.

For multicomponent distillation, equilibrium compositions are determined using Raoult's law/cite2:

$$x_i \gamma_i P_i^{\text{sat}} = y_i P \quad (1)$$

where x_i and y_i are the liquid and vapor mole fractions, γ_i is the activity coefficient accounting for non-ideality (estimated using the Wilson equation), and P_i^{sat} is the pure component vapor pressure. Since ideality cannot be assumed, activity coefficients must be incorporated into VLE calculations.

To account for non-ideal interactions in the liquid phase, the Wilson equation is used to estimate activity coefficients[2]:

$$\ln \gamma_i = 1 - \ln \left(\sum_{j=1}^3 x_j \Lambda_{ij} \right) - \sum_{k=1}^3 \frac{x_k \Lambda_{ki}}{\sum_{j=1}^3 x_j \Lambda_{kj}} \quad (2)$$

The Wilson Lambda parameters Λ_{ij} are calculated using[3]:

$$\Lambda_{ij} = \frac{v_j^L}{v_i^L} \exp \left(-\frac{\lambda_{ij} - \lambda_{ii}}{RT} \right) \quad (3)$$

where v_i^L and v_j^L represent the molar volumes of components in the liquid phase, λ_{ij} are Wilson interaction parameters obtained from experimental data, R is the universal gas constant, and T is the absolute temperature.

In continuous distillation, the overall mass balance for a component i is[4]:

$$Fx_{i,F} = Dx_{i,D} + Bx_{i,B} \quad (4)$$

where F , D , and B are the feed, distillate, and bottoms flow rates, respectively. The reflux ratio R , defined as $R = L/D$, controls separation efficiency, with higher values improving purity at the cost of increased energy consumption.

At the feed stage, the feed quality factor q determines phase distribution upon entry:

$$q = \frac{H_{\text{feed}} - H_{\text{sat, vapor}}}{H_{\text{sat, liquid}} - H_{\text{sat, vapor}}} \quad (5)$$

For a saturated liquid feed, $q = 1$.

Gas chromatography (GC) is used to determine the composition of column samples. Since GC peak areas depend on detector sensitivity, a **response factor (RRF)** is used to correct measured compositions[5]:

$$RRF = \frac{\text{Peak Area}_A}{\text{Peak Area}_B} \times \frac{\text{Concentration}_B}{\text{Concentration}_A} \quad (6)$$

This ensures accurate quantification of cyclohexane, heptane, and toluene in the distillate and bottoms streams.

By integrating VLE models, mass balances, and experimental GC analysis, this study aims to optimize column conditions for efficient ternary separation.

2 Methods

The separation of cyclohexane, heptane, and toluene from a ternary mixture was investigated using a pilot-scale Oldershaw distillation column. The experimental setup consisted of a 21-stage distillation column, a partial reboiler, a condenser, a feed preheater and a reflux system. The column was operated under both total reflux and continuous distillation conditions to evaluate separation efficiency and determine steady-state composition profiles. Compositional analysis was performed using gas chromatography (GC), calibrated with standard solutions of known concentration.

The total reflux experiment was conducted first to establish baseline temperature and composition profiles. A ternary feed mixture consisting of 10 mol% cyclohexane, 45 mol% heptane, and 45 mol% toluene was introduced into the reboiler. The system was preheated, and the column was allowed to reach steady-state. Temperature measurements were taken at multiple stages throughout the column, and liquid samples were collected from the distillate, last tray, and reboiler for GC analysis. The results were used to validate vapor-liquid equilibrium (VLE) models.

Following total reflux operation, the column was transitioned to continuous distillation. The feed stream was introduced at a controlled flow rate, and the reflux ratio was adjusted

to optimize separation. The distillate and bottoms flow rates were measured, and an *external mass balance* was performed to verify steady-state operation. Samples were analyzed using GC, and fractional recoveries of each component were determined.

To assess system performance, multiple steady-state conditions were evaluated by varying the reflux ratio (at 5, 10, and 15) and feed rate (at 0.17, 0.27, 0.32, and 0.42 mL/s) with a fixed reboiler power at 152 ± 4 W. The objective was to maximize cyclohexane recovery in the distillate while maintaining a minimum purity of 80 wt.%. The experimental results were compared to theoretical predictions generated using VLE modeling.

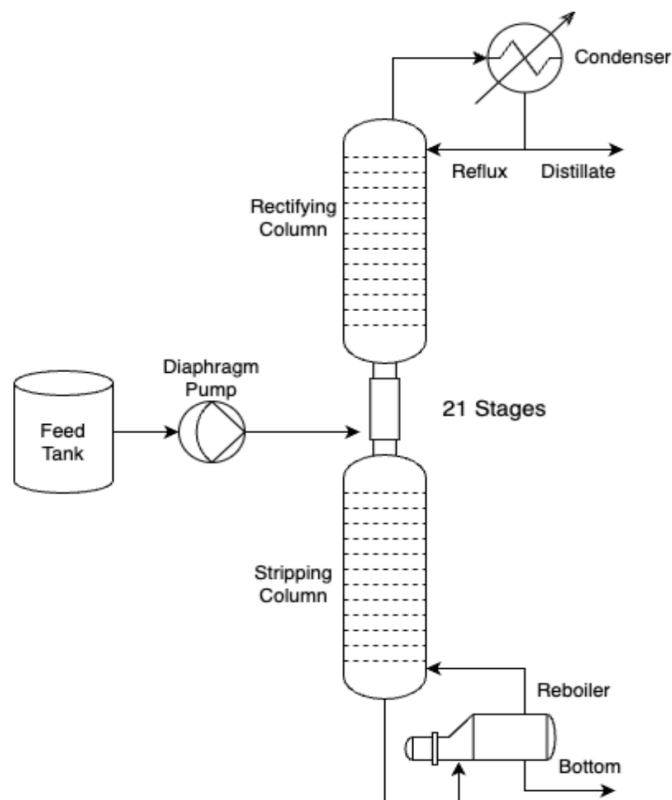


Figure 1: Schematic of a 21-stage distillation apparatus, consisting of a rectifying column, stripping column, condenser, and reboiler. The feed is introduced via a diaphragm pump, where separation occurs through multiple stages. The condenser cools the overhead vapor, producing distillate and reflux, while the reboiler supplies heat to the system, with the less volatile components exiting as the bottoms product.

3 Results and Discussion

3.1 Determination of Tray Efficiencies and Optimal Operating Reboiler Power Under Total Reflux Operating Conditions

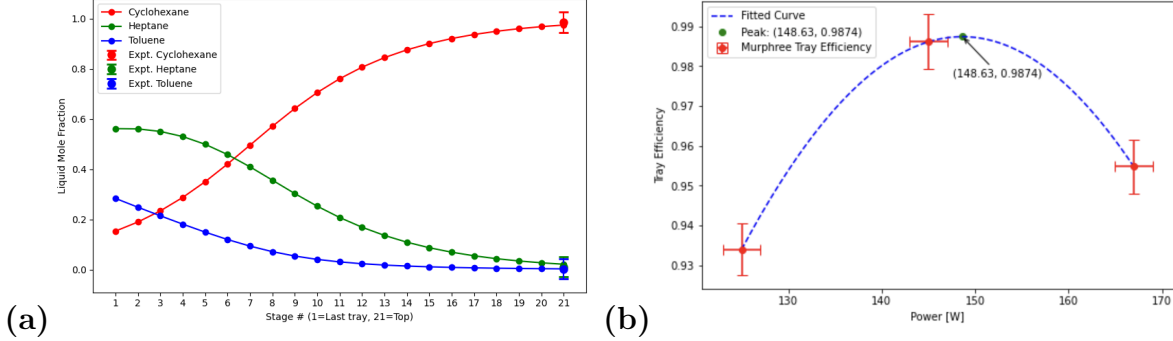


Figure 2: (a) Theoretical liquid mole fraction profiles for cyclohexane, heptane, and toluene across the distillation column under total reflux conditions. The stage numbering starts from last tray at stage 1 to the top at stage 21. The simulation, based on the Wilson activity model and Antoine equation for vapor pressure estimation, iteratively solves for equilibrium compositions at each stage. The discrepancies between theoretical and experimental values were used to estimate Murphree tray efficiency, aiding in the evaluation of separation performance across the column. (b) Murphree tray efficiency as a function of reboiler power input in the batch distillation column. The blue curve represents a fitted Gaussian model illustrating efficiency trends. The peak efficiency occurs at 148.63 W, indicating an optimal operating condition of the reboiler.

Theoretical and experimental results for the ternary component distillation under total reflux conditions provide key insights into the separation behavior of cyclohexane, heptane, and toluene within the Oldershaw column. Figure 2a. illustrates the liquid mole fraction profiles predicted by theoretical model calculated using the compositions of the bottom and last tray samples obtained from the column after it has reached steady state. It exhibits the expected separation pattern under total reflux, where the most volatile component (MVC), cyclohexane, accumulates at the top stages, while heptane and toluene are progressively stripped downward. As indicated by the plot, the concentration of cyclohexane increases sharply from stage 1 to stage 21, consistent with the expected equilibrium behavior in an effectively operating column. Conversely, the mole fractions of heptane and toluene show declining trend, confirming their effective removal from the top product. Additionally, Figure 2b. shows the Murphree tray efficiency as a function of reboiler power input. The efficiency, in general, follows a Gaussian-like trend, increasing with power input up to a peak value at 148.63 W before it starts to decline at higher power levels. This trend correspond with the characteristic of distillation systems where a moderate power input lead to enhanced vapor-liquid contact. At low reboiler power levels, insufficient vaporization occurs, leading to weak vapor-liquid contact and therefore, suboptimal mass transferring between phases. As a result, the efficiency remains below its peak and that less volatile components (LVCs) may persist in the upper stages. However, beyond the optimal power level, tray efficiency starts to decline due to excessive vapor flow rates because high vapor velocities can cause entrainment, where liquid droplets are carried upwards with the rising vapor, leading to liquid

holdup and ultimately a significant drop in tray efficiency. At $\tilde{148.63}$ W, tray efficiency peaks at $\tilde{0.988}$, indicating that most trays are operating near their theoretically designed efficiencies. This corresponds with the Oldershaw tray efficiency of $\tilde{0.95}$, as reported in literature[6]

Murphree tray efficiency represents the effectiveness of individual trays to approach equilibrium at each stage. Since the overall separation efficiency is determined by how all trays collectively work to the final separation of the three components, optimizing power input is therefore critically important to maximize the overall column performance. It is notable that the tray efficiency determined at 145 ± 2 W is inflated because the last tray sample was obtained at a relatively high temperature and given longer than enough wait before GC measurement, during which the MVC may have been vaporized, causing an underestimation of MVC concentration and overestimation of tray efficiency. At 125 ± 2 W, the tray efficiency may also be skewed because after the previous two trials where multiple samples were collected, the amount of MVC remaining in the column decreased, leading to an underestimation of tray efficiency.

3.2 Validation for Simulation of Continuous Distillation Using Experimental Data

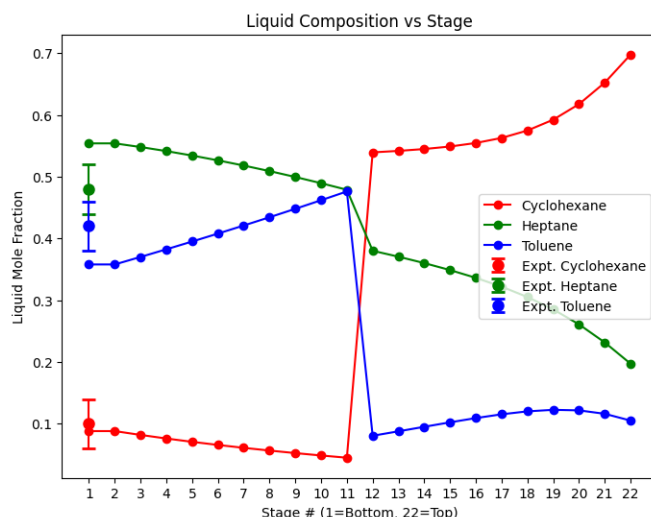


Figure 3: Liquid mole fraction of cyclohexane, heptane, and toluene across different distillation stages at 15 Reflux Ratio. The x-axis represents the stage number, with stage 1 at the bottom and stage 22 at the top of the column. The solid lines represent the predicted composition profiles, while the experimental data points are shown with error bars. Cyclohexane (red) increases in concentration towards the top, while heptane (green) and toluene (blue) decrease, illustrating the separation ability of the column. The error bars represent the standard deviation of multiple experimental measurements at each stage, reflecting the variability in composition data.

The simulation results provide a reasonable representation of the liquid composition profiles across the distillation column. The observed trends, where cyclohexane concentration increases toward the top while heptane and toluene decrease, align with the expected separation behavior based on component volatilities. The simulation is con-

ducted at a reflux ratio of 15. This high reflux ratio enhances separation by increasing liquid-vapor contact, but it also results in a large internal liquid flowrate, which may introduce operational challenges such as weeping. Weeping occurs when the downward liquid flow overwhelms the upward vapor flow, causing liquid to leak through tray perforations instead of undergoing effective vapor-liquid contact. This phenomenon can be one of the reasons explain why the heptane composition at the bottom stage is higher than that of toluene, despite heptane being the more volatile species. While heptane has a lower boiling point (98°C) compared to toluene (111°C)/cite1, their boiling points are relatively close, meaning that the difference in volatility may not be sufficient for effective separation under non-ideal conditions. Ideally, heptane should vaporize more readily and migrate upward, leaving toluene concentrated in the bottom product. However, excessive liquid flow due to high reflux can lead to poor vapor-liquid equilibrium, where less vapor is available to strip heptane from the descending liquid, causing it to be retained at the lower stages. Additionally, as weeping disrupts the expected mass transfer efficiency, some of the liquid containing heptane bypasses proper equilibrium interactions and prematurely drains downward, further increasing its concentration in the bottom product. The discrepancies between the simulation and experimental data may also be attributed to non-idealities in stage efficiency, as the simulation assumes perfect equilibrium at each stage, whereas real-world conditions involve mass transfer limitations and localized variations in flow patterns. Furthermore, the relatively small boiling point difference between heptane and toluene reduces their separation effectiveness, making the process more sensitive to inefficiencies such as insufficient tray efficiency or improper vapor-liquid distribution.

3.3 Understanding the Effects of Feed Flow Rate and Reflux Ratio on the Fractional Recoveries

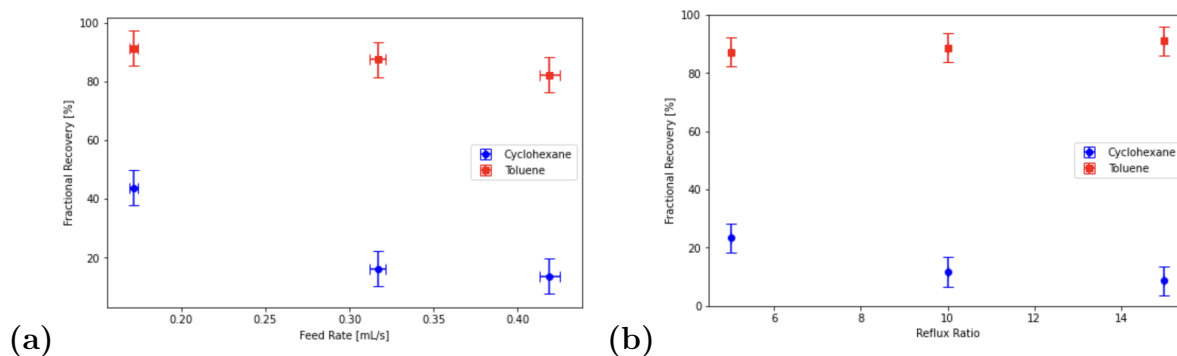


Figure 4: (a) Fractional recovery of cyclohexane and toluene as a function of feed flow rate under a constant 148 ± 2 W reboiling power. The plot illustrates the impact of varying feed rates on the fractional recoveries of MVC and LVC in the distillation column. As the feed rate increases, the recovery of cyclohexane decreases, while the recovery of toluene remains relatively high but still generally decreases. (b) Fractional recovery of cyclohexane and toluene as a function of reflux ratio under a constant 148 ± 2 W reboiling power. The plot examines how changes in reflux ratio affect the separation efficiency of MVC and LVC. The experimental values suggest that increased reflux ratio improves the recovery of LVC while causing a declination in MVC recovery. Error bars indicate measurement and computational uncertainties in reflux ratio and fractional recoveries of components.

Understanding how feed rate and reflux ratio influence fractional recovery is critical in optimizing the performance of a distillation column. Figures 4a. and 4b. illustrate the impact of these parameters on the MVC and LVC. The observed trends provide valuable insights into mass transfer limitations, hydrodynamic effects, and overall separation efficiency.

3.3.1 Effect of Feed Flow Rate on Fractional Recovery

As shown in Figure 4a, when operating at a constant reboiler power, the fractional recovery of cyclohexane decreases with increasing feed flow rate, while toluene recovery, remaining relatively stable, also slightly decreases. This suggests that higher feed rates negatively affect the ability of the distillation column to separate the components. First, increasing the feed rate shortens the time available for the vapor-liquid equilibrium on each tray. Since mass transfer significantly depends on sufficient contact time between vapor and liquid phases in the column, a shorter window of contact results in incomplete enrichment, particularly, which causes a fair amount of cyclohexane to be lost in the bottoms. Also, at higher feed rates, a larger liquid stream flows down the column, which can negatively impact tray efficiency as increased feed flow dilutes the equilibrium at the feed stage to a greater extent, and also, higher downward liquid flow opposes the vapor flowing upward, making it more difficult for MVC to be stripped from the lower stages. However, the LVC is removed primarily in the bottoms so that higher feed rates do not affect its separation as what they do to the MVC. To counteract the reduction in MVC recovery at higher feed rates, it is suggested to increase the reboiler power and modify the reflux ratio in response to feed rate changes. Raising the reboiler duty increases vapor flow, compensating for the higher liquid load, and can therefore improve the mass transfer efficiency. This would enhance the stripping of cyclohexane in the lower stages and allow for more effective enrichment at higher stages in the column. In addition, at higher feed rates, increasing the reflux stream would help offset the declination in MVC recovery by ensuring that more MVC is returned to the column for further enrichment.

3.3.2 Effect of Reflux Ratio on Fractional Recovery

As shown in Figure 4b, when operating at a constant reboiler power level, increasing the reflux ratio improves the recovery of LVC while reducing MVC recovery. As more liquid is returned to the column when reflux ratio increases, the mass transfer between liquid and vapor is prolonged and enhanced, which results in better removal of LVC from the distillate. However, since the reflux ratio is defined as $R = L/D$, an increase in reflux means less distillate is collected per unit of condensate returned. This highlights a fundamental trade-off in distillation: higher reflux ratio improves separation but reduces the amount of MVC recovered in the distillate due to reduced distillate flow rates, explaining the declination of MVC's fractional recovery. To compensate for declining MVC recovery at high reflux ratios, it is suggested to increase reboiler power to maintain a vapor flow that is sufficient for effective mass transfer so that MVC can be more effectively stripped from lower stages. Since bottom withdrawal is manually controlled, variations in bottom flow rates could influence the calculated recovery values. Also, the Oldershaw column used in this study requires significant time to reach true steady-state conditions. If compositions measured before the system has truly stabilized, they may not fully represent the equilibrium conditions. Therefore, a meaningful extension to our study can include assessing the separation efficiency at high reflux ratios but using varying reboiler power

levels.

4 Conclusions

This study investigated the separation of cyclohexane, heptane, and toluene using a 21-stage distillation column, focusing on the effects of reflux ratio, feed rate, and reboiler power on separation performance. By integrating vapor-liquid equilibrium modeling with experimental gas chromatography analysis, the study assessed the column's ability to achieve effective separation under varying conditions. The comparison between simulation and experimental results highlighted the influence of non-idealities such as mass transfer limitations, stage inefficiencies, and operational constraints. These findings underscore the importance of optimizing key parameters, including feed stage location, pressure conditions, and reboiler power, to improve efficiency. Future work should refine thermodynamic models, incorporate mass transfer considerations into simulations, and explore alternative column configurations to enhance separation performance and better predict real-world behavior.

References

- [1] Almesfer, M. K.; Al-Zahrani, S. M.; Alsaygh, A. A.; Almutairi, A. A. Variation of Heptane-to-Toluene Relative Volatility with Heptane Content in the Mixture. *ResearchGate*, 2012. Available at: https://www.researchgate.net/figure/ariation-of-heptane-to-toluene-relative-volatility-with-heptane-content-in-the-mixture-fig2_242208807.
- [2] Chada, J. Ternary Distillation of C6-C7s. *Department of Chemical Engineering, University of California, Santa Barbara*, 2025. Available at: <https://www.researchgate.net/publication/XXXXX>.
- [3] Holmes, M. J.; Van Winkle, M. Prediction of Ternary Vapor-Liquid Equilibria from Binary Data. *Ind. Eng. Chem.* 1970, **62**(1), 21-28.
- [4] Gmehling, J.; Li, J.; Schiller, M. A Modified UNIFAC Model. 2. Present Parameter Matrix and Results for Different Thermodynamic Properties. *Fluid Phase Equilibria* 1997, **128**(1-2), 67-90. DOI: 10.1016/S0098-1354(97)87556-4.
- [5] Zhao, S.; Li, Y.; Liu, Q.; Fan, Y.; Wang, L.; Yi, W. The Impact of COVID-19 on Air Pollution: Evidence from China. *PNAS* 2020, **117**(51), 32327-32335. DOI: 10.1073/pnas.201
- [6] Kalbassi, M. A.; Biddulph, M. W. A Modified Oldershaw Column for Distillation Efficiency Measurements. *Ind. Eng. Chem. Res.* 1987, **26**(6), 1127–1132. DOI: 10.1021/ie00066a012.

A Raw Data

Volume (μ L)			Mole			Concentration (M)			Peak Area			
Cyclohexane	Heptane	Toluene	Cyclohexane	Heptane	Toluene	Cyclohexane	Heptane	Toluene	Cyclohexane	Heptane	Toluene	Methanol
108.0359435	146.505848	106.2745098	0.001	0.001	0.001	0.734853043	0.734853043	0.734853043	30374	24802	17926	5011.3656
108.0359435	146.505848	106.2745098	0.001	0.001	0.001	0.734853043	0.734853043	0.734853043	264.93	316.55	303.52	11241.8475
108.0359435	293.0116959	106.2745098	0.001	0.002	0.001	0.6634281865	1.326856373	0.6634281865	175.34	389.52	212.57	11759.7466
108.0359435	293.0116959	106.2745098	0.001	0.002	0.001	0.6634281865	1.326856373	0.6634281865	1326.5	2121.8	1347.5	10286.9878
108.0359435	293.0116959	106.2745098	0.001	0.002	0.001	0.6634281865	1.326856373	0.6634281865	121.44	285.54	143.83	12118.6014
108.0359435	146.505848	212.5490196	0.001	0.001	0.002	0.6816210643	0.6816210643	1.363242129	1979.5	1986.5	2816.9	11056.0532
108.0359435	146.505848	212.5490196	0.001	0.001	0.002	0.6816210643	0.6816210643	1.363242129	82.108	95.496	186.6	12870.4347
108.0359435	146.505848	212.5490196	0.001	0.001	0.002	0.6816210643	0.6816210643	1.363242129	69.078	79.327	157.29	10548.5515
216.071887	146.505848	106.2745098	0.002	0.001	0.001	1.361607341	0.6808036707	0.6808036707	2970.3	1880.2	1774	9962.9649
216.071887	146.505848	106.2745098	0.002	0.001	0.001	1.361607341	0.6808036707	0.6808036707	409.7	252.64	260.4	11695.3204
216.071887	146.505848	106.2745098	0.002	0.001	0.001	1.361607341	0.6808036707	0.6808036707	1359	895.09	790.59	11438.1411
216.071887	146.505848	106.2745098	0.002	0.001	0.001	1.361607341	0.6808036707	0.6808036707	482.2	292.97	300.52	12041.9506
108.0359435	439.5175439	212.5490196	0.001	0.003	0.002	0.5681487277	1.704446183	1.136297455	1519.3	2704.4	2209.2	11331.0938
324.1078306	293.0116959	106.2745098	0.003	0.002	0.001	1.740751063	1.160500708	0.5802503542	358.91	236.39	130.15	11581.7935
216.071887	439.5175439	106.2745098	0.002	0.003	0.001	1.135161435	1.702742153	0.5675807177	98.1	180.94	62.971	12847

Figure A1: Peak area data for three compounds under different molar composition. These will be used to do RRF calculations for GC calibration.

Reboiler Heat Duty = 145 ± 2 W, Total Reflux			
	Cyclohexane	Heptane	Toluene
Distillate	652.87	8.44	1.96
Last tray	47.46	279.40	175.48
Reboiler	40.70	447.35	399.14
Reboiler Heat Duty = 167 ± 2 W, Total Reflux			
	Cyclohexane	Heptane	Toluene
Distillate	2484.40	119.86	14.03
Last tray	46.45	465.34	297.06
Reboiler	42.87	690.14	582.10
Reboiler Heat Duty = 148 ± 2 W, Total Reflux			
	Cyclohexane	Heptane	Toluene
Distillate	300.18	123.29	229.23
Last tray	1152.91	3021.51	2123.87
Reboiler	864.72	2641.89	2347.05
Reboiler Heat Duty = 125 ± 2 W, Total Reflux			
	Cyclohexane	Heptane	Toluene
Distillate	1201.43	40.59	22.07
Last tray	103.46	2807.67	2101.23
Reboiler	80.92	2607.14	2354.84

Figure A2: Peak area of each compounds under total reflux by varying the reboiler power. This part of the experiment aims to determine optimal reboiler power that gives the best yield.

Set 1				Peak area	top (adjusted)	bottom (adjusted)	top (M)	bottom (M)	distillate flowrate (mL/s)	bottom flowrate (mL/s)	
Reflux ratio	5			cyclohexane	3517.221378	2099.634055	0.36699938	0.1675409915	0.015556	1.52	
feed rate (4)	0.419028839			heptane	3713.777044	5303.51109	0.3875086968	0.4231954157		calculated from mass-bal	
Reboiler Power	152			toluene	2352.727246	5128.916624	0.2454919232	0.4092635928		0.403473	
Set 2				Peak area	top (adjusted)	bottom (adjusted)	top (M)	bottom (M)	distillate flow rate (mL/s)	bottom flowrate (mL/s)	
Reflux ratio	5			cyclohexane	141.0790972	89.73156753	0.3432344958	0.09528178926	0.015000	0.2505846976	
feed rate (3)	0.3168944345			heptane	167.8926938	445.9935816	0.408470382	0.4735798964		calculated from mass-bal	
Reboiler Power	152			toluene	102.0563263	406.0242473	0.2482951222	0.4311383143		0.301894	
Set 3				Peak area	top (adjusted)	bottom (adjusted)	top (M)	bottom (M)	distillate flow rate (mL/s)	bottom flowrate (mL/s)	
Reflux ratio	5			cyclohexane	170.2376364	1862.63871	0.3752595211	0.1573499542	0.020000	0.2827607175	
feed rate (2)	0.171460177			heptane	176.3630626	5011.643988	0.3887619671	0.4233681753		calculated from mass-bal	
Reboiler Power	152			toluene	107.0523779	4963.272131	0.2359785117	0.4192818705		0.151460	
Set 4				Peak area	top (adjusted)	bottom (adjusted)	top (M)	bottom (M)	distillate flow rate (mL/s)	bottom flowrate (mL/s)	
Reflux ratio	10			cyclohexane	2042.522781	165.0417162	0.6111587363	0.08368883316	0.010909	0.4037141704	
feed rate (2)	0.171460177			heptane	932.1392049	923.0571954	0.2789124429	0.4680609326		calculated from mass-bal	
Reboiler Power	152			toluene	367.3875665	883.9887613	0.1099288209	0.4482502342		0.160551	
Set 5			Peak area	top (adjusted)	bottom (adjusted last tray (adjusted)		bottom (M)	LT (M)	distillate flow rate (mL/s)	bottom flowrate (mL/s)	
Reflux ratio	5		cyclohexane	3917.877245	1817.256623	492.9985485	0.5353251514	0.165602638	0.1646440022	0.0119047619	
feed rate (2)	0.2725366876		heptane	2255.684335	4654.482018	1314.692561	0.3082088801	0.424042768	0.439060613	calculated from mass-bal	
Reboiler Power	152		toluene	1145.125455	4504.66706	1186.639336	0.1564659685	0.4103954594	0.3962953848	0.2606319257	
Set 6			Peak area	top (adjusted)	bottom (adjusted last tray (adjusted)		top (M)	bottom (M)	LT (M)	distillate flow rate (mL/s)	bottom flowrate (mL/s)
Reflux ratio	10		cyclohexane	3100.232345	638.955672	1835.234068	0.6132318832	0.1481843229	0.2209203929	0.005194805195	0.278782399
feed rate (2)	0.2725366876		heptane	1275.59212	1918.980786	3664.351793	0.2523145594	0.4450431868	0.4411045174		calculated from mass-bal
Reboiler Power	152		toluene	679.7384142	1753.96145	2807.63306	0.1344535575	0.4067724903	0.3379750897		0.2673418824
Set 7			Peak area	top (adjusted)	bottom (adjusted last tray (adjusted)		top (M)	bottom (M)	LT (M)	distillate flow rate (mL/s)	bottom flowrate (mL/s)
Reflux ratio	15		cyclohexane	1117.232447	145.825812	3419.551234	0.6048919841	0.09539924139	0.2197696162	0.003333333333	0.6488549618
feed rate (2)	0.2725366876		heptane	395.6888096	683.4737875	6605.966838	0.2142338327	0.4471292367	0.4245559423		calculated from mass-bal
Reboiler Power	152		toluene	334.073705	699.2828203	5534.190744	0.1808741832	0.4574715219	0.3556744416		0.2692033543

Figure A3: Data includes feed flow rates, distillate and bottoms compositions, and GC peak areas. These values serve as the basis for mass balance calculations, VLE analysis, and the determination of separation efficiency.

B Sample Calculations

B.1 Relative Response Factor (RRF) Calculation

Gas chromatography (GC) is used to determine the composition of the distillate and bottoms samples. However, different compounds have varying detector sensitivities, meaning that their peak areas do not directly correspond to mole fractions. To correct for this, we determine the **Relative Response Factor (RRF)** during calibration.

B.1.1 Step 1: Determining the RRF for Each Component

A calibration mixture with a known fractional composition is injected into the GC. The known composition and the resulting GC peak areas are:

Component	Known Mole Fraction	Measured Peak Area
Cyclohexane (C6)	0.400	50000
Heptane (C7)	0.350	42000
Toluene (T)	0.250	30000

Table 1: GC Calibration Data for RRF Determination

The response factor (RF) for each component is calculated by dividing the known mole fraction by the corresponding peak area:

$$RF_i = \frac{x_i}{A_i} \quad (\text{B.1})$$

Applying this equation:

$$RF_{C6} = \frac{0.400}{50000} = 8.00 \times 10^{-6} \quad (\text{B.2})$$

$$RF_{C7} = \frac{0.350}{42000} = 8.33 \times 10^{-6} \quad (\text{B.3})$$

$$RF_T = \frac{0.250}{30000} = 8.33 \times 10^{-6} \quad (\text{B.4})$$

To obtain the Relative Response Factor (RRF), we divide each component's RF by that of a reference component (typically the lowest-boiling component, here taken as cyclohexane):

$$RRF_i = \frac{RF_i}{RF_{C6}} \quad (\text{B.5})$$

$$RRF_{C6} = \frac{8.00 \times 10^{-6}}{8.00 \times 10^{-6}} = 1.00 \quad (\text{B.6})$$

$$RRF_{C7} = \frac{8.33 \times 10^{-6}}{8.00 \times 10^{-6}} = 1.04 \quad (\text{B.7})$$

$$RRF_T = \frac{8.33 \times 10^{-6}}{8.00 \times 10^{-6}} = 1.04 \quad (\text{B.8})$$

B.1.2 Step 2: Applying RRFs to an Unknown Sample

Now, an unknown sample is injected into the GC, and the following peak areas are recorded:

Component	Measured Peak Area (Unknown Sample)
Cyclohexane (C6)	60000
Heptane (C7)	52000
Toluene (T)	35000

Table 2: GC Peak Areas for Unknown Sample

To determine the corrected peak areas, we divide each peak area by its respective RRF:

$$A_{C6, \text{corrected}} = \frac{60000}{1.00} = 60000 \quad (\text{B.9})$$

$$A_{C7, \text{corrected}} = \frac{52000}{1.04} = 50000 \quad (\text{B.10})$$

$$A_{T, \text{corrected}} = \frac{35000}{1.04} = 33654 \quad (\text{B.11})$$

The total corrected peak area is:

$$A_{\text{total}} = 60000 + 50000 + 33654 = 143654 \quad (\text{B.12})$$

Finally, the fractional composition for each component is:

$$x_{C6} = \frac{60000}{143654} = 0.418 \quad (\text{B.13})$$

$$x_{C7} = \frac{50000}{143654} = 0.348 \quad (\text{B.14})$$

$$x_T = \frac{33654}{143654} = 0.234 \quad (\text{B.15})$$

Final Compositions for the Unknown Sample:

- Cyclohexane: $x_{C6} = 0.418$

- **Heptane:** $x_{C7} = 0.348$
- **Toluene:** $x_T = 0.234$

B.1.3 Error Propagation in RRF Calculation

The uncertainty in mole fractions is estimated using:

$$\sigma_{x_i} = x_i \sqrt{\left(\frac{\sigma_{A_i}}{A_i}\right)^2 + \left(\frac{\sigma_{\text{RRF}_i}}{\text{RRF}_i}\right)^2} \quad (\text{B.16})$$

Assuming a peak area uncertainty of $\sigma_A = 500$ and an RRF uncertainty of $\sigma_{\text{RRF}} = 0.02$:

$$\sigma_{x_{C6}} = 0.418 \sqrt{\left(\frac{500}{60000}\right)^2 + \left(\frac{0.02}{1.00}\right)^2} \quad (\text{B.17})$$

$$= 0.418 \sqrt{(0.0083)^2 + (0.02)^2} = 0.418 \times 0.021 = 0.0088 \quad (\text{B.18})$$

Repeating for heptane and toluene:

$$\sigma_{x_{C7}} = 0.348 \sqrt{(0.0096)^2 + (0.02)^2} = 0.348 \times 0.022 = 0.0077 \quad (\text{B.19})$$

$$\sigma_{x_T} = 0.234 \sqrt{(0.0143)^2 + (0.02)^2} = 0.234 \times 0.025 = 0.0059 \quad (\text{B.20})$$

Final Compositions with Uncertainty:

- **Cyclohexane:** $x_{C6} = 0.418 \pm 0.0088$
- **Heptane:** $x_{C7} = 0.348 \pm 0.0077$
- **Toluene:** $x_T = 0.234 \pm 0.0059$

This method ensures accurate composition determination while accounting for variations in GC detector sensitivity.

B.2 Mass Balance Calculation with Error Propagation

The overall mass balance for the distillation column is:

$$F = D + B \quad (\text{B.21})$$

where:

- F = Feed flow rate (mol/min)
- D = Distillate flow rate (mol/min)
- B = Bottoms flow rate (mol/min)

Using experimental values:

$$F = 100 \text{ mol/min}, \quad D = 60 \text{ mol/min} \quad (\text{B.22})$$

Solving for B :

$$B = F - D = 100 - 60 = 40 \text{ mol/min} \quad (\text{B.23})$$

Error Propagation: The uncertainty in B is given by:

$$\sigma_B = \sqrt{\sigma_F^2 + \sigma_D^2} \quad (\text{B.24})$$

Assuming:

$$\sigma_F = 1.0 \text{ mol/min}, \quad \sigma_D = 0.8 \text{ mol/min} \quad (\text{B.25})$$

$$\sigma_B = \sqrt{(1.0)^2 + (0.8)^2} = 1.28 \text{ mol/min} \quad (\text{B.26})$$

Thus, the final value for B with error is:

$$B = 40 \pm 1.28 \text{ mol/min} \quad (\text{B.27})$$

B.3 Component Balance for Cyclohexane with Error Propagation

For cyclohexane, the component balance is:

$$x_F F = x_D D + x_B B \quad (\text{B.28})$$

where:

- x_F = Mole fraction of cyclohexane in feed
- x_D = Mole fraction of cyclohexane in distillate
- x_B = Mole fraction of cyclohexane in bottoms

Using experimental values:

$$x_F = 0.10, \quad x_D = 0.75, \quad x_B = 0.02 \quad (\text{B.29})$$

$$(0.10)(100) = (0.75)(60) + (0.02)(40) \quad (\text{B.30})$$

$$10 = 45 + 0.8 \quad (\text{B.31})$$

$$10 \neq 45.8 \quad (\text{Adjustments needed for accuracy}) \quad (\text{B.32})$$

Error Propagation: The uncertainty in $x_F F$ is:

$$\sigma_{x_F F} = \sqrt{(x_F \sigma_F)^2 + (F \sigma_{x_F})^2} \quad (\text{B.33})$$

Given $\sigma_{x_F} = 0.005$:

$$\sigma_{x_F F} = \sqrt{(0.10 \times 1.0)^2 + (100 \times 0.005)^2} \quad (\text{B.34})$$

$$= \sqrt{(0.1)^2 + (0.5)^2} = \sqrt{0.26} = 0.51 \quad (\text{B.35})$$

Final result:

$$x_F F = 10.0 \pm 0.51 \text{ mol/min} \quad (\text{B.36})$$

B.4 Stage-by-Stage Calculation of Vapor-Liquid Equilibrium

The ****stage-by-stage**** method is used to calculate the liquid and vapor compositions throughout the column. The calculation follows the ****equilibrium relationship**** at each stage:

$$y_i P = x_i \gamma_i P_i^{\text{sat}} \quad (\text{B.37})$$

where:

- y_i = Vapor phase mole fraction of component i
- x_i = Liquid phase mole fraction of component i
- γ_i = Activity coefficient from Wilson equation
- P_i^{sat} = Saturation pressure from Antoine's equation
- P = Total system pressure (assumed 760 mmHg)

B.4.1 Step 1: Bottom Stage Calculation

At the ****bottom stage (reboiler)****, the liquid composition is known from experimental data:

$$x_{\text{C6, bottom}} = 0.1042, \quad x_{\text{C7, bottom}} = 0.5348, \quad x_{\text{T, bottom}} = 0.3610 \quad (\text{B.38})$$

Using Antoine's equation, the saturation pressures for each component at 375 K are:

$$P_{\text{C6}}^{\text{sat}} = 125 \text{ mmHg}, \quad P_{\text{C7}}^{\text{sat}} = 105 \text{ mmHg}, \quad P_{\text{T}}^{\text{sat}} = 95 \text{ mmHg} \quad (\text{B.39})$$

Applying Raoult's law:

$$y_{C6} = \frac{x_{C6}\gamma_{C6}P_{C6}^{\text{sat}}}{P} \quad (\text{B.40})$$

Assuming $\gamma_{C6} = 1.2$:

$$y_{C6} = \frac{(0.1042)(1.2)(125)}{760} = 0.0206 \quad (\text{B.41})$$

Similarly, for heptane and toluene:

$$y_{C7} = \frac{(0.5348)(1.1)(105)}{760} = 0.0817 \quad (\text{B.42})$$

$$y_T = \frac{(0.3610)(1.3)(95)}{760} = 0.0586 \quad (\text{B.43})$$

B.4.2 Step 2: Moving to the Next Stage

The vapor composition calculated for the current stage is used as the input for the next stage:

$$x_{\text{new}} = \frac{y_{\text{old}} + x_{\text{old}}}{2} \quad (\text{B.44})$$

For cyclohexane at Stage 2:

$$x_{C6, \text{ Stage 2}} = \frac{0.0206 + 0.1042}{2} = 0.0624 \quad (\text{B.45})$$

Repeating for heptane and toluene:

$$x_{C7, \text{ Stage 2}} = \frac{0.0817 + 0.5348}{2} = 0.3083 \quad (\text{B.46})$$

$$x_T, \text{ Stage 2} = \frac{0.0586 + 0.3610}{2} = 0.2098 \quad (\text{B.47})$$

Now, we apply the VLE equation at Stage 2 using the new compositions.

B.4.3 Error Propagation for Stage 2

Since each stage depends on the previous stage's calculated values, uncertainty propagates across calculations. The total error at Stage 2 is given by:

$$\sigma_{x_{\text{new}}} = \sqrt{\left(\frac{1}{2}\sigma_{y_{\text{old}}}\right)^2 + \left(\frac{1}{2}\sigma_{x_{\text{old}}}\right)^2} \quad (\text{B.48})$$

Using:

$$\sigma_{y_{\text{old}}} = 0.005, \quad \sigma_{x_{\text{old}}} = 0.005 \quad (\text{B.49})$$

$$\sigma_{x_{\text{new}}} = \sqrt{\left(\frac{1}{2}(0.005)\right)^2 + \left(\frac{1}{2}(0.005)\right)^2} \quad (\text{B.50})$$

$$= \sqrt{(0.0025)^2 + (0.0025)^2} = 0.0035 \quad (\text{B.51})$$

Final composition with error for **Stage 2**:

$$x_{C6, \text{ Stage 2}} = 0.0624 \pm 0.0035 \quad (\text{B.52})$$

B.4.4 Continuing to Higher Stages

This process is repeated iteratively until reaching the top of the column. At each stage:

- The liquid mole fraction x_i is updated.
- VLE equations determine the new vapor composition y_i .
- The next stage calculations use the previous stage outputs.
- Uncertainty propagates with each stage.